

1 **A combined *in vitro/in silico* approach to identifying off-target receptor toxicity**

2

3 Joseph Leedale^{1*†}, Kieran J. Sharkey¹, Helen E. Colley², Áine M. Norton³, David Peeney³,
4 Chantelle L. Mason⁴, Jean G. Sathish^{3,5}, Craig Murdoch², Parveen Sharma^{3*}, Steven D.
5 Webb⁴

6

7 ¹EPSRC Liverpool Centre for Mathematics in Healthcare, Dept. of Mathematical Sciences,
8 University of Liverpool, Liverpool, L69 7ZL, UK

9 ²School of Clinical Dentistry, University of Sheffield, Sheffield, S10 2TA, UK

10 ³Dept. of Molecular and Clinical Pharmacology, University of Liverpool, Liverpool, L69
11 3GE, UK

12 ⁴Dept. of Applied Mathematics, Liverpool John Moores University, Liverpool, L3 3AF, UK

13 ⁵Immuno and Molecular Toxicology, Drug Safety Evaluation, Bristol-Myers Squibb, 1
14 Squibb Drive, New Brunswick, NJ, 08903, USA

15

16 ***Correspondence**

17 For theoretical work:

18 Joseph Leedale (†lead contact)
19 EPSRC Liverpool Centre for Mathematics in Healthcare
20 Dept. of Mathematical Sciences
21 University of Liverpool
22 Liverpool L69 7ZL
23 United Kingdom
24 Tel: +44 (0)151 794 4049
25 Email: j.leedale@liverpool.ac.uk

26

27 For experimental work:

28 Parveen Sharma
29 MRC Centre for Drug Safety Science
30 Dept. of Molecular and Clinical Pharmacology
31 University of Liverpool
32 Liverpool L69 3GE
33 United Kingdom
34 Tel: +44 (0)151 795 0149
35 Email: psharma@liverpool.ac.uk

36 **Summary**

37 Many xenobiotics can bind to off-target receptors and cause toxicity via the dysregulation of
38 downstream transcription factors. Identification of subsequent off-target toxicity in these
39 chemicals has often required extensive chemical testing in animal models. An alternative,
40 integrated *in vitro/in silico* approach for predicting toxic off-target functional responses is
41 presented to refine *in vitro* receptor identification and reduce the burden on *in vivo* testing. As
42 part of the methodology, mathematical modelling is used to mechanistically describe
43 processes that regulate transcriptional activity following receptor-ligand binding informed by
44 transcription factor signalling assays. Critical reactions in the signalling cascade are identified
45 to highlight potential perturbation points in the biochemical network that can guide and
46 optimise additional *in vitro* testing. A physiologically-based pharmacokinetic model provides
47 information on the timing and localisation of different levels of receptor activation informing
48 whole-body toxic potential resulting from off-target binding.

49 **Introduction**

50 Many drugs are designed to interact specifically with cell surface, cytoplasmic or nuclear
51 receptors in order to produce a beneficial therapeutic effect. However, drugs can often bind to
52 and interact with receptors that are not their intended targets and such “off-target” binding
53 may cause what is now often termed a molecular initiating event (MIE); e.g. receptor
54 activation of toxicological relevance that may ultimately lead to an adverse drug reaction
55 (ADR) (Edwards & Aronson, 2000, Guengerich, 2011, Muller & Milton, 2012). In many
56 instances, ADRs can lead to significant morbidity and mortality as well as contributing to
57 high levels of attrition during drug development (Lazarou et al., 1998, Pirmohamed et al.,
58 2004). This can primarily be attributed to an incomplete understanding of the molecular
59 mechanism of action of a given compound and the lack of ability to predict which receptors
60 may be activated unintentionally.

61 The sole use of *in vitro*-based experimental strategies in the early stages of drug development
62 and chemical testing is important but can lead to an unreliable and incomplete understanding
63 of reactions (Coleman, 2011). Therefore, often considerable numbers of animals are used to
64 screen out chemicals that may cause off-target toxicity with figures for the UK reporting that
65 306,000 *in vivo* toxicology safety procedures were performed in 2014 (Home Office, 2015).
66 In addition, the chemical industry used almost 345,000 animals in the EU for toxicological or
67 other safety evaluations (European Commission, 2013) and in the USA 3-6 million fish are
68 used annually for whole effluent toxicity testing (Scholz et al., 2013). Furthermore,
69 pharmacokinetics and pharmacodynamics are significantly different between animal models
70 and humans diminishing their effectiveness in detecting toxicity through pre-clinical studies
71 (Lauschke et al., 2016). There is therefore a clear need to develop scientific approaches to
72 identify toxicologically relevant off-target receptor binding in order to reduce the burden of
73 animal use in toxicity testing. The development of a more ethical, non-animal toolkit for
74 initial chemical toxicological assessment using an integrated human-based *in vitro/in silico*

75 system would enhance current strategies and may even expedite the drug development
76 pipeline.

77 In intracellular signalling, ligand/receptor interactions lead to the activation of a distinct set of
78 transcription factors, the effects of which tend to be tissue specific. Several companies now
79 offer transcription factor activation profiling platforms and so it is possible to identify and
80 catalogue the transcription factor activation profiles of toxicologically relevant receptors
81 upon binding of their known ligands/drugs. It is assumed that transcription factor profiles
82 generated from off-target receptor activation of any given drug can be matched against
83 known ligand/receptor transcription profiles in order to predict which specific receptor (or
84 class of receptors) has been activated in the initial off-target MIE. However, when testing off-
85 target profiles of new compounds, the resulting transcription profile may not precisely match
86 a known receptor (e.g. partial agonism or the binding of multiple receptors) and therefore a
87 method of refinement is required to narrow the subset of off-target receptors. Our approach
88 aims to refine the *in vitro* receptor identification process for off-target receptors by using
89 information about the changes in receptor-mediated transcription factor activity following the
90 introduction of a given compound and integrating this information with predictive *in silico*
91 models and analysis. This approach allows for the identification of relevant perturbations in
92 the transcription factor signalling pathway that signify the binding of a receptor or smaller
93 range of receptors as well as other points of interest in the transcription factor signalling
94 network that can contribute towards and guide subsequent off-target receptor identification.

95 Translating the wealth of knowledge on network interactions of cellular components to
96 dynamic models is generally limited by the amount of available quantitative information to
97 accompany these relationships such as molecular amounts and reaction rates. However,
98 qualitative dynamic network modelling can be used to compare with routinely generated
99 semi-quantitative experimental time-course data, where perturbations can provide valuable
100 information about the system. *In silico* modelling of this type then provides a platform for the
101 refinement of more quantitative (parameter based) modelling (Fisher et al., 2013). In such a
102 scenario, the network modelling method of Petri nets provide an effective tool, particularly in
103 the complex, stochastic framework of molecular biological pathways (Chaouiya, 2007,
104 Heiner et al., 2008, Heidary et al., 2015). Petri nets are often used to model multiple species
105 and reactions without defining large quantities of unknown parameters, as modelling
106 emphasis is upon network topology and relative amounts of species rather than specific
107 reaction rates. This emphasis on network structure can then be translated to methods such as
108 flux balance analysis and metabolic control analysis without knowledge of rate constants, as
109 was shown for the switching of the metabolic pathway in *E. Coli* (Edwards et al., 2001,
110 Kitano, 2002).

111 The identification of off-target receptor binding alone for a given compound is insufficient to
112 predict significant off-target toxicity and so we aim to provide additional information to
113 support and refine the subsequent evaluation of toxic potential. This is achieved by

114 translating knowledge of receptor binding properties and relative distribution of the receptor
115 throughout the body to a whole-body response to the xenobiotic. This approach utilises a
116 physiologically based pharmacokinetic (PBPK) model adapted specifically for describing
117 receptor activation throughout the body following compound exposure. A PBPK model is a
118 mechanistic, multi-compartment mathematical model that describes the time-course
119 dynamics and overall kinetics of an administered drug dose throughout the organism of
120 interest. PBPK models integrate the physicochemical properties of the substance with the
121 specific physiology of the organism such that the evolution of the ADME (Absorption,
122 Distribution, Metabolism and Excretion) processes can be simulated *in silico*. Drug/substance
123 properties include tissue affinity, membrane permeability, enzymatic stability etc., while the
124 organism/system component include such properties as organ mass/volume and blood flow
125 (Rowland et al., 2011). PBPK modelling is used in this work to couple the pharmacokinetics
126 of a drug to dose-response parameters with the associated off-target receptor in different
127 tissues in order to generate spatio-temporal dynamics of the off-target receptor activation.

128 **Results**

129 *Development of the signalling pathway model*

130 As proof of concept, an *in silico* model of the histamine H1 receptor signalling pathway was
131 formulated. This pathway was chosen due to the well understood intracellular signalling
132 interactions involved upon receptor stimulation and the existence of a known off-target
133 partial agonist, lisuride (Bakker et al., 2004). The H1 receptor is a G-protein coupled receptor
134 that, upon activation, leads to dissociation of $G\alpha_{q/11}$ and the $G\beta\gamma$ complex. $G\alpha_{q/11}$ activates
135 phospholipase C β (PLC β) leading to hydrolysis of phosphatidylinositol 4,5-bisphosphate
136 (PIP $_2$) and the formation of inositol triphosphate (IP $_3$) and diacylglycerol (DAG) (Bakker et
137 al., 2001, Sandal et al., 2013). IP $_3$ mediates transient intracellular calcium release from the
138 endoplasmic reticulum (Shah et al., 2015) that eventually mediates activation of nuclear
139 factor of activated T-cells (NFAT) (Macian, 2005), cAMP response element-binding protein
140 (CREB) (Johannessen & Moens, 2007) and myocyte enhancer factor-2 (Mef2) transcription
141 factors (Lu et al., 2000). Diacylglycerol simultaneously activates protein kinase C (PKC) and
142 this phosphorylates I κ B kinase (IKK), ultimately leading to nuclear factor kappa-light-chain-
143 enhancer of activated B cells (NF κ B) transcription factor activation (La Porta & Comolli,
144 1997). The $G\beta\gamma$ complex also plays a role in histamine signal transduction; regulating many
145 effectors including adenylate cyclase (AC) (Maruko et al., 2005) and phosphoinositide 3
146 kinase (PI3K) (Gautam et al., 1998). AC mediates the subsequent activation of protein kinase
147 A via cyclic adenosine monophosphate (cAMP) leading to CREB phosphorylation and
148 transcription factor activation (Mosenden & Taskén, 2011). PI3K mediates the activation of
149 Akt, NF- κ B and activating transcription factor 2 (ATF2) (Bence et al., 1997, Breitwieser et
150 al., 2007). To provide semi-quantitative information for the relative transcription factor
151 dynamics as described above, we assayed pathway perturbations using a luciferase reporter-
152 based transcription factor array to calibrate the fold increase expected of key signalling

153 outputs upon stimulation with an agonist. These transcription factors were identified as
154 NFAT, NF- κ B, CREB, Mef2, and ATF2. Incubation of H1 receptor expressing HeLa cells
155 with histamine showed considerable activation of these transcription factors (**Table 1**).

156 A stochastic Petri net model of the histamine H1 receptor signalling pathway was formulated
157 based on existing knowledge of the pathway and network interactions with the five critical
158 transcription factors determined to be activated following ligand binding. The pathway in this
159 proof of concept provides an illustrative example of what should ultimately form part of a
160 larger cell signalling model that incorporates the complexity of the known toxicological
161 receptors and associated transcription factors in the proposed methodology. The H1 Petri net
162 includes the key dynamic molecular species and appropriate network interactions that are
163 activated during ligand-binding-induced signalling. This pathway is depicted using the
164 modified Edinburgh Pathway Notation (mEPN) format (Freeman et al., 2010) in Figure 1 and
165 directly corresponds to the layout of the Petri net. All rates are equal such that all stochastic
166 transitions are equally likely to fire but are effectively modulated by the concentration of
167 upstream reactants in a mass action process. Time is interpreted qualitatively reflecting the
168 relative order of events. Varying quantities in the mathematical model such as the amount of
169 ligand introduced (“dose”) and the total amounts of system species (i.e. moieties of active and
170 inactive states for each protein) modulates the scale of transcriptional activity regulation and
171 as such, these values were optimised to correlate with the experimental signalling assays.
172 This optimisation was carried out by assuming a large-scale continuum approximation of the
173 Petri net to a system of ordinary differential equations (ODEs) and fitting to the
174 corresponding transcription factor output data (Figure 2). It should be noted that the optimal
175 parameter set is non-identifiable for such a large system with relatively few data points to fit.
176 However, this issue was the precise motivation for the combined Petri net/metabolic control
177 analysis approach which is well suited to understanding the relative impact of small
178 perturbations on the transcription factors of interest and prioritise network connectivity
179 information in favour of accurate predictions of parameters and dynamics (Koch et al., 2010).
180 Corresponding pathway reactions, moieties and ODEs can be found in the supplementary
181 material. In addition to providing static information on the network interactions of the
182 signalling pathway and relative changes in steady state activity following receptor activation,
183 Petri nets can also be used to simulate transient temporal dynamics providing further dynamic
184 information on the relative order and scale of transcriptional regulation (Figure 3) following a
185 receptor-ligand binding event. However, it is clear that more data would be required for one
186 to relate this dynamic output to the biological context, and validate any potential predictions
187 about transient dynamics.

188 *Analysis of network perturbations to identify off-target responses*

189 The identification of significant pathway reactions upstream of transcription was achieved
190 using metabolic control analysis (MCA), which is a mathematical technique that tests the
191 sensitivity of a given variable to network perturbations (Kacser & Burns, 1973, Heinrich &

192 Rapoport, 1974). Specifically, scaled MCA concentration control coefficients provide the
 193 ratio between a relative measure of change in the steady state of a system variable as affected
 194 by perturbations in network reaction rates. In our illustrative H1 example model, MCA
 195 coefficients were calculated for each transcription factor that was experimentally determined
 196 to show significant change in activity following binding of the H1 receptor (Figure 4). The
 197 rows of the heat map in Figure 4 correspond to the numbered reactions as indicated in the
 198 supplementary material. MCA not only points to the direct regulation of gene transcription as
 199 critical to H1-associated transcriptional activity (white patches in Figure 4), but to other
 200 reactions within the cascade, upstream of the transcription factors and downstream of the
 201 target receptor. For example, in this system the transcriptional activity of Mef2 is sensitive to
 202 relatively distant biochemical reactions, such as the rate of calcium release from the
 203 endoplasmic reticulum (24% of maximum sensitivity provided by perturbation of Mef2
 204 transcription rate). Also, the model suggests that the transcriptional activity of ATF2 is more
 205 sensitive to perturbations in PIP2 synthesis than it is to regulation of the BTK:PIP3 complex
 206 that directly activates ATF2 by phosphorylation.

207 The identification of these sensitive perturbation points within the signalling pathway model
 208 provide information beyond the transcription factor activity measurements found
 209 experimentally, which allows for more optimised, directed experimental designs for receptor
 210 identification, if initial screening fails to identify the off-target receptor. For example, for a
 211 given compound that was shown to regulate Mef2 transcriptional activity but did not interact
 212 with the H1 receptor, this model would inform a proposal to screen for receptors that are
 213 known to interact with biochemical reactions identified as being sensitive, such as calcium
 214 release, during MCA.

215 ***Translation to tissue scales using a PBPK model***

216 Following an *in silico* identification of an off-target receptor, extrapolation to the study of
 217 potential *in vivo* toxicity can be performed using a PBPK model. For our illustrative example,
 218 receptor binding properties are provided by EC₅₀ dose-response curves for the off-target H1
 219 agonist, lisuride (Figure 5A), and measurements of the corresponding binding affinity, K_d
 220 (Bakker et al., 2004). The dose-response curves were estimated by fitting the following
 221 equation to the dose-response data:

$$222 \text{ Response\%} = \text{Min} + \frac{(\text{Max} - \text{Min})L^n}{EC_{50}^n + L^n}, \quad (1)$$

223 for ligand concentration L . The optimised parameter values are given in **Table 2**. In order to
 224 provide tissue-specific responses we also used Western blot measurements of relative H1
 225 EC₅₀ values using,

$$226 EC_{50i} = \frac{K_d EC_{50}}{R_i(K_d + EC_{50}) - EC_{50}}$$

227 where i denotes the i^{th} tissue, K_d is the dissociation equilibrium constant for lisuride and
228 R_i is a measure of receptor abundancy in tissue i (see Table 3). For simplicity, this model
229 assumes that the same amount of receptor binding is required to achieve 50% response in
230 each tissue in the absence of any other information, particularly as the response measured is
231 proximal to receptor binding attenuating any potential amplification effects arising from
232 potential signalling cascades in different tissues (Kenakin, 2009). For further information
233 regarding this derivation see the supplementary material.

234 In order to simulate the pharmacokinetics of lisuride throughout the body, physicochemical
235 properties of the compound were required which were obtained from previously published
236 measurements. These properties include lipophilicity, whether the drug is neutral/acid/base,
237 solubility (obtained from the DrugBank database (Wishart et al., 2006)), molecular weight
238 (O'Neil, 2013), acid dissociation constant (Meloun et al., 2005) and effective permeability
239 (Winiwarter et al., 1998). The time-course dynamics simulated by the PBPK model for drug
240 concentration in each tissue compartment of the body were then coupled to receptor binding
241 properties and relative receptor expression in tissues to provide a predictive temporal
242 response throughout the body. This response can be produced for any dosage regime and
243 various methods of administration such as intravenous, oral and inhalation. The PBPK model
244 was based on the form derived by Peters (2008). The model was optimised for lisuride
245 physicochemical and binding properties and the H1 receptor distribution throughout the
246 different tissues. Example lisuride response kinetics following both intravenous (IV) and oral
247 administrations can be found in Figure 6. The IV dose of 25 $\mu\text{g}/\text{mL}$ used in Figure 6 was the
248 same as that used in a previous pharmacokinetic study for relevance (Krause et al., 1991).
249 This experimental data was also the IV data used to optimise the PBPK model to recapitulate
250 the lisuride dynamics in the venous blood compartment and also simulate corresponding oral
251 profiles as per the methodology described by Peters (2008). The oral dose of 0.1 mg chosen
252 for the PBPK model was deemed relevant by matching previous pharmacological studies
253 (Koizumi et al., 1985, Al-Sereiti & Turner, 1989). The dynamic response of the H1 receptor
254 is visualised over time as a solution to equation (1) with tissue-specific EC_{50} values for the
255 pharmacokinetics of lisuride (L) in different parts of the body. Both IV and oral
256 administration simulations are plotted to also highlight the impact of delivery route. This is
257 particularly pertinent in this case where we are studying a receptor which has a relatively
258 high concentration in the gastrointestinal tract. IV administration results in relatively high
259 receptor stimulation in the liver, brain, small intestine and colon at earlier times whereas oral
260 administration results in a more gradual accumulation in these tissues and the receptors in the
261 colon are stimulated at a near maximal level for a relatively long time after oral ingestion.
262 These simulations allow us to compare how the off-target response varies throughout the
263 body over time depending on the pharmacokinetics of the drug coupled with physiologically
264 relevant receptor availability and receptor binding information. Such information is
265 potentially useful to determine whether or not an identified off-target agonist is likely to elicit

266 an off-target receptor response in an area of high target density based on its physicochemical
267 properties.

268 **Discussion**

269 Adverse drug reactions (ADRs) are a major cause of patient morbidity, mortality and drug
270 attrition during development (Pirmohamed et al., 2004). This can be attributed to a poor
271 understanding of the mechanisms underlying the toxic response and also to a lack of current
272 tools for the prediction of a toxic outcome. Animal models have a limited scope and data
273 obtained using such models may not be ideal for ascertaining toxicity seen in humans. As
274 such, computational systems biology models can be essential tools to improve chemical
275 reaction predictivity (Krewski et al., 2010). In this study, we describe a new *in silico*
276 modelling method that can be used to enhance current knowledge of pathway perturbations in
277 order to provide a new toxicity-testing paradigm based on human biology. In this method,
278 chemical-mediated activation of transcription factors and intracellular signalling pathway
279 molecules were used as readouts to inform and drive a pathway-based *in silico* approach to
280 identify possible upstream receptor(s) engaged by such chemicals. *In vitro* data was then used
281 to inform a PBPK *in silico* modelling platform to understand and rank risk of toxicity at
282 tissue, organ and whole-body levels over time. Key to this integrative approach was the
283 coupling of *in vitro* experimental techniques and advanced *in silico* modelling to create a
284 unique resource that, with further development and parameterisation, could be used to predict
285 the off-target toxicity of compounds that can then inform and direct more focussed *in vivo*
286 experimentation.

287 Mathematical modelling was used in order to mechanistically describe the processes that lead
288 to regulation of transcriptional activity following the binding of ligand to receptor. This was
289 achieved by designing a signalling pathway model that represented all the relevant processes
290 and biochemical reactions downstream of ligand binding, culminating in the regulation of
291 transcription. We have established a novel *in vitro/in silico* approach using data from assays
292 measuring transcription factor activation and chemically-induced perturbations of
293 intracellular signalling pathways to inform *in silico* pathway modelling. This unbiased
294 pathway-led approach uses computational simulations to identify causality between receptor
295 activation and pathway perturbations to aid identification of the upstream receptor/s engaged
296 by the initial MIE. As proof of concept, an *in silico* Petri net model of the histamine H1
297 receptor-signalling pathway was formulated with the off-target compound, lisuride. The
298 output of this system provides semi-quantitative temporal dynamics for the entire pathway
299 that can be used to investigate system perturbations, simulate experiments and provide
300 structural pathway predictions. *In vitro* reporter assay data was then used to parameterise and
301 validate the model, and the identification of critical candidate perturbation points was
302 achieved using metabolic control analysis (MCA). Signalling pathway models can be
303 purposely used in this methodology to provide a library of MCA coefficients for a range of
304 transcription factors associated with receptor binding and toxicity, and guide further

305 experimentation. In the example shown, calcium release from the endoplasmic reticulum and
306 PIP2 synthesis are highlighted as important upstream events for the transcriptional activity of
307 Mef2 and ATF2. If a new compound is shown to induce the activity of these transcription
308 factors but the receptor responsible is not identified via screening for instance, further testing
309 could be guided towards targets that modulate these upstream processes. This illustrates the
310 feasibility of this approach in directing further experimentation towards relevant pathway
311 mechanisms or receptor clusters during the process of receptor identification via focussed *in*
312 *vitro* assay testing.

313 *In vitro* to *in vivo* extrapolations of whole-body consequences of receptor binding was
314 explored using PBPK modelling. The structure of PBPK models typically revolves around
315 the anatomical structure of the organism with different organs and tissues of varying
316 perfusion rates being separated into distinct compartments. These compartments are then
317 coupled through the circulation, whose arterial and venous flow is described to connect the
318 organs in a physiological way. Entrance points (e.g. absorption) of the model depend on the
319 drug administration method (e.g. inhalation, ingestion, injection) while exit points (e.g.
320 excretion) are generally described via the kidneys and intestine. The flow kinetics of the
321 model determine distribution, while metabolism occurs in the liver and intestine. The inherent
322 physiological basis distinguishes true PBPK models from their PK model counterparts that
323 usually simplify the physiology to fewer hypothetical compartments of different flow rates,
324 driven by the data/process of interest, such that they are often more tractable analytically. In
325 contrast, PBPK models are generally more complex but are designed to have a better global
326 representation such that valid extrapolations can be made and disparate experimental data can
327 be integrated during model parameterisation. In this way, PBPK models are less reliant on
328 data-fitting to obtain appropriate values for equation parameters and essentially the same
329 model (with appropriate modifications) can be suitably applied in many different
330 pharmacological scenarios for quantitative risk assessment and therapy optimisation.

331 PBPK model simulations are increasingly being used in pharmacology, in both academia and
332 industry, in order to provide important predictions of the pharmacokinetic properties and
333 toxic potential of new drugs at an early stage in drug development (Zhao et al., 2011, Jones &
334 Rowland-Yeo, 2013, Tsamandouras et al., 2015). This type of *in silico* testing can offer a
335 quicker, cheaper and more ethical alternative method when compared to traditional *in vivo*
336 experiments performed. Ideally, both experimental and computational methods are used
337 harmoniously to provide a cycle of information and enhanced knowledge iteration as the
338 accuracy of PBPK models inevitably rely on quality experimental data to calibrate rates
339 within the differential equations. In the method reported here, physicochemical properties of
340 the chemical are combined with tissue specific receptor expression and EC₅₀ data to predict
341 time-course dynamics of the chemical concentrations in each tissue, as well as tissue level
342 receptor activation responses to that chemical. These predictions can be produced for any
343 dosage regime and various methods of administration. In the example study of the off-target
344 partial agonist of the histamine H1 receptor, lisuride, the combination of lisuride

345 pharmacokinetics and relative H1 receptor distribution throughout the body allowed us to
346 predict that the dose response would be most significant in the brain, liver and
347 gastrointestinal system. In this case example, these results are supported by prior knowledge
348 of the compound and receptor although the modelling was done agnostic of such prior *in vivo*
349 findings. In particular, receptor response localised to the brain is somewhat expected since
350 lisuride is primarily a psychotherapeutic drug, affecting dopamine and serotonin regulation
351 (Marona-Lewicka et al., 2002). Lisuride is primarily metabolised in the liver, where there is
352 relatively high expression of histamine receptors. There is also high receptor expression in
353 the gastrointestinal tract due to the role of histamine in intestinal secretion and motility (Leurs
354 et al., 1995, Sander et al., 2006). Furthermore, lisuride administration in patients with
355 Parkinson's disease has been associated with gastrointestinal side effects (Ebadi & Pfeiffer,
356 2004). Although relative response rates have been quantified by the model in different parts
357 of the body at different times, to translate what such a response directly represents in the
358 context of toxicity and clinical relevance is very complicated, and restricted in this
359 methodology, establishing a challenge beyond the scope of this paper. However, these PBPK-
360 based extrapolations do allow us to generate predictive data relevant to risk assessment and
361 further translation to toxicity at the organ and whole-body levels for off-target receptor
362 perturbations. The output provided by this method is intended to identify toxic potential and
363 guide subsequent *in vitro* and *in vivo* experimentation to organs of interest/importance.

364 The operating parameters of the approach are circumscribed by the extent of current
365 knowledge regarding receptors and their function. This represents a potential limitation of the
366 strategy, although the mathematically-driven signalling pathway model has the potential to
367 identify novel, uncharacterised receptor targets. The challenge of identifying sensitive
368 perturbation points within large-scale networks of receptor signalling pathways required that
369 a semi quantitative network-based approach must be used. This inevitably limits the amount
370 of predictive, dynamic information that can be extrapolated and caution must be exercised
371 such that the utility of mathematical models is preserved by acknowledging the relevant
372 application that stimulated its design. The approach is experimental (with elements of
373 modelling and extrapolation to assess and rank toxicological risk) and does not incorporate
374 prediction of receptor binding based on chemical or receptor structures. The strength of the
375 methodology is predicated on currently available, validated experimental methods as it does
376 not require the development of new, untested technologies and relies on sound criteria-based
377 selection of receptors, and quantifying receptor function and binding using established
378 experimental techniques. Future work requires the development of multiple pathway models
379 based on training chemical data as well as the integration of pathways, which should be
380 optimised and validated with non-training data. Furthermore, the current PBPK framework
381 can be extended to ensure improved predictive potential by incorporating mechanistic tissue
382 models, catering for a wider range of chemicals and capturing population level responses.
383 More work is also needed to translate tissue-level receptor activation responses to measures
384 of toxicity such as relevant biomarkers. Carefully calculated person-to-person variation and

385 covariances within organism-related parameters would also allow for the prediction of a
386 population response whereby different individuals within a sample population may exhibit
387 different levels of exposure and therefore associated toxicity from the same dosage levels.
388 The combined *in vitro/in silico* approach of this study has shown how the multidisciplinary,
389 iterative process of systems biology can be applied to direct experiments, optimise the utility
390 of generated data and challenge and refine theoretical modelling in order to improve methods
391 for detecting and predicting toxicity caused by compounds that bind to off-target receptors.

392

393 **Acknowledgments**

394 JL, KJS and SDW acknowledges funding support from the Liverpool Centre for Mathematics
395 in Healthcare (EPSRC grant: EP/N014499/1). All authors acknowledge funding support from
396 the NC3Rs CRACK-IT Challenge 18: Targeting off-targets award.

397 **Author Contributions**

398 JL contributed to the mathematical modelling and wrote the manuscript; KJS and CLM
399 contributed to the mathematical modelling; HEC and CM contributed to the design of the
400 experimental work; AMN and DP performed the experiments; JGS designed the research; PS
401 contributed to, designed and performed the experimental work; SDW contributed to the
402 mathematical modelling and directed the research. All authors read and approved the final
403 manuscript.

404 **Declaration of Interests**

405 The authors declare no competing interests.

406

407

408 **References**

409 Al-Sereiti M.R. and Turner P. (1989). The effects of lisuride, terguride and bromocriptine on
410 intraocular pressure (IOP). *Br. J. Clin. Pharmacol.* 27: 159-163.

411
412 Bakker R.A., Schoonus S.B.J., Smit M.J., Timmerman H. and Leurs R. (2001). Histamine
413 H1-receptor activation of nuclear factor- κ B: roles for G β γ -and G α q/11-subunits in
414 constitutive and agonist-mediated signaling. *Mol. Pharmacol.* 60: 1133-1142.

415
416 Bakker R.A., Weiner D.M., Ter Laak T., Beuming T., Zuiderveld O.P., Edelbroek M.,
417 Hacksell U., Timmerman H., Brann M.R. and Leurs R. (2004). 8R-lisuride is a potent
418 stereospecific histamine H1-receptor partial agonist. *Mol. Pharmacol.* 65: 538-549.

419
420 Bence K., Ma W., Kozasa T. and Huang X.-Y. (1997). Direct stimulation of Bruton's tyrosine
421 kinase by Gq-protein α -subunit. *Nature* 389: 296-299.

422
423 Breitwieser W., Lyons S., Flenniken A.M., Ashton G., Bruder G., Willington M., Lacaud G.,
424 Kouskoff V. and Jones N. (2007). Feedback regulation of p38 activity via ATF2 is essential
425 for survival of embryonic liver cells. *Genes Dev.* 21: 2069-2082.

426
427 Chaouiya C. (2007). Petri net modelling of biological networks. *Briefings in bioinformatics*
428 8: 210-219.

429
430 Coleman R.A. (2011). Human tissue in the evaluation of safety and efficacy of new
431 medicines: a viable alternative to animal models? *ISRN pharmaceuticals* 2011.

432
433 Ebadi M. and Pfeiffer R.F. (2004). *Parkinson's Disease*, (CRC Press).

434
435 Edwards I.R. and Aronson J.K. (2000). Adverse drug reactions: definitions, diagnosis, and
436 management. *The Lancet* 356: 1255-1259.

437
438 Edwards J.S., Ibarra R.U. and Palsson B.O. (2001). In silico predictions of Escherichia coli
439 metabolic capabilities are consistent with experimental data. *Nat. Biotechnol.* 19: 125-130.

440
441 European Commission (2013). *Seventh Report on the Statistics on the Number of Animals*
442 *used for Experimental and other Scientific Purposes in the Member States of the European*
443 *Union.*

444

445 Fisher C.P., Plant N.J., Moore J.B. and Kierzek A.M. (2013). QSSPN: dynamic simulation of
446 molecular interaction networks describing gene regulation, signalling and whole-cell
447 metabolism in human cells. *Bioinformatics* 29: 3181-3190.

448

449 Freeman T.C., Raza S., Theocharidis A. and Ghazal P. (2010). The mEPN scheme: an
450 intuitive and flexible graphical system for rendering biological pathways. *BMC Syst. Biol.* 4:
451 65.

452

453 Gautam N., Downes G.B., Yan K. and Kisselev O. (1998). The G-protein $\beta\gamma$ complex. *Cell.*
454 *Signal.* 10: 447-455.

455

456 Guengerich F.P. (2011). Mechanisms of drug toxicity and relevance to pharmaceutical
457 development. *Drug Metab. Pharmacokinet.* 26: 3-14.

458

459 Heidary Z., Ghaisari J., Moein S., Naderi M. and Gheisari Y. (2015). Stochastic Petri Net
460 Modeling of Hypoxia Pathway Predicts a Novel Incoherent Feed-Forward Loop Controlling
461 SDF-1 Expression in Acute Kidney Injury.

462

463 Heiner M., Gilbert D. and Donaldson R. (2008). Petri nets for systems and synthetic biology.
464 *Formal methods for computational systems biology, (Springer):* 215-264.

465

466 Heinrich R. and Rapoport T.A. (1974). A Linear Steady-State Treatment of Enzymatic
467 Chains. *The FEBS Journal* 42: 97-105.

468

469 Home Office (2015). Annual Statistics of Scientific Procedures on Living Animals Great
470 Britain 2014.

471

472 Johannessen M. and Moens U. (2007). Multisite phosphorylation of the cAMP response
473 element-binding protein (CREB) by a diversity of protein kinases. *Front Biosci* 12: e32.

474

475 Jones H.M. and Rowland-Yeo K. (2013). Basic concepts in physiologically based
476 pharmacokinetic modeling in drug discovery and development. *CPT: pharmacometrics &*
477 *systems pharmacology* 2: 1-12.

478

479 Kacser H. and Burns J.A. (1973). The Control of Flux. *Symp. Soc. Exp. Biol.* 27: 65-104.

480

481 Kenakin T. (2009). *A pharmacology primer: theory, application and methods, (Academic*
482 *Press).*

483
484 Kitano H. (2002). Systems biology: a brief overview. *Science* 295: 1662-1664.

485
486 Koch I., Reisig W. and Schreiber F. (2010). Modeling in systems biology: the Petri net
487 approach, (Springer Science & Business Media).

488
489 Koizumi K., Aono T. and Kurachi K. (1985). The effect of lisuride hydrogen maleate on
490 anterior pituitary hormones, oestradiol and cortisol in normal and hyperprolactinaemic
491 women. *European Journal of Obstetrics & Gynecology and Reproductive Biology* 20: 19-26.

492
493 Krause W., Mager T., Kühne G., Duka T. and Voet B. (1991). The pharmacokinetics and
494 pharmacodynamics of lisuride in healthy volunteers after intravenous, intramuscular, and
495 subcutaneous injection. *Eur. J. Clin. Pharmacol.* 40: 399-403.

496
497 Krewski D., Acosta Jr D., Andersen M., Anderson H., Bailar III J.C., Boekelheide K., Brent
498 R., Charnley G., Cheung V.G. and Green Jr S. (2010). Toxicity testing in the 21st century: a
499 vision and a strategy. *Journal of Toxicology and Environmental Health, Part B* 13: 51-138.

500
501 La Porta C.A. and Comolli R. (1997). PKC-dependent modulation of I κ B alpha-NF κ B
502 pathway in low metastatic B16F1 murine melanoma cells and in highly metastatic BL6 cells.
503 *Anticancer Res.* 18: 2591-2597.

504
505 Lauschke V.M., Hendriks D.F.G., Bell C.C., Andersson T.B. and Ingelman-Sundberg M.
506 (2016). Novel 3D Culture Systems for Studies of Human Liver Function and Assessments of
507 the Hepatotoxicity of Drugs and Drug Candidates. *Chem. Res. Toxicol.*

508
509 Lazarou J., Pomeranz B.H. and Corey P.N. (1998). Incidence of adverse drug reactions in
510 hospitalized patients: a meta-analysis of prospective studies. *JAMA* 279: 1200-1205.

511
512 Leurs R., Smit M. and Timmerman H. (1995). Molecular pharmacological aspects of
513 histamine receptors. *Pharmacol. Ther.* 66: 413-463.

514
515 Lu J., McKinsey T.A., Nicol R.L. and Olson E.N. (2000). Signal-dependent activation of the
516 MEF2 transcription factor by dissociation from histone deacetylases. *Proceedings of the
517 National Academy of Sciences* 97: 4070-4075.

518
519 Macian F. (2005). NFAT proteins: key regulators of T-cell development and function. *Nature
520 Reviews Immunology* 5: 472-484.

521

522 Marona-Lewicka D., Kurrasch-Orbaugh D.M., Selken J.R., Cumbay M.G., Lisnicchia J.G.
523 and Nichols D.E. (2002). Re-evaluation of lisuride pharmacology: 5-hydroxytryptamine_{1A}
524 receptor-mediated behavioral effects overlap its other properties in rats. *Psychopharmacology*
525 164: 93-107.

526
527 Maruko T., Nakahara T., Sakamoto K., Saito M., Sugimoto N., Takuwa Y. and Ishii K.
528 (2005). Involvement of the $\beta\gamma$ subunits of G proteins in the cAMP response induced by
529 stimulation of the histamine H1 receptor. *Naunyn-Schmiedeberg's Arch. Pharmacol.* 372:
530 153-159.

531
532 Meloun M., Syrový T. and Vrana A. (2005). The thermodynamic dissociation constants of
533 haemanthamine, lisuride, metergoline and nicergoline by the regression analysis of
534 spectrophotometric data. *Anal. Chim. Acta* 543: 254-266.

535
536 Mosenden R. and Taskén K. (2011). Cyclic AMP-mediated immune regulation—overview of
537 mechanisms of action in T cells. *Cell. Signal.* 23: 1009-1016.

538
539 Muller P.Y. and Milton M.N. (2012). The determination and interpretation of the therapeutic
540 index in drug development. *Nature reviews Drug discovery* 11: 751-761.

541
542 O'Neil M.J. (2013). *The Merck Index: An Encyclopedia of Chemicals, Drugs, and*
543 *Biologicals*, (Royal Society of Chemistry).

544
545 Peters S.A. (2008). Evaluation of a generic physiologically based pharmacokinetic model for
546 lineshape analysis. *Clin. Pharmacokinet.* 47: 261-275.

547
548 Pirmohamed M., James S., Meakin S., Green C., Scott A.K., Walley T.J., Farrar K., Park
549 B.K. and Breckenridge A.M. (2004). Adverse drug reactions as cause of admission to
550 hospital: prospective analysis of 18 820 patients. *BMJ* 329: 15-19.

551
552 Rowland M., Peck C. and Tucker G. (2011). Physiologically-based pharmacokinetics in drug
553 development and regulatory science. *Annu. Rev. Pharmacol. Toxicol.* 51: 45-73.

554
555 Sandal M., Paltrinieri D., Carloni P., Musiani F. and Giorgetti A. (2013). Structure/function
556 relationships of phospholipases C Beta. *Current Protein and Peptide Science* 14: 650-657.

557
558 Sander L.E., Lorentz A., Sellge G., Coeffier M., Neipp M., Veres T., Frieling T., Meier P.N.,
559 Manns M.P. and Bischoff S.C. (2006). Selective expression of histamine receptors H1R,
560 H2R, and H4R, but not H3R, in the human intestinal tract. *Gut* 55: 498-504.

561
562 Scholz S., Sela E., Blaha L., Braunbeck T., Galay-Burgos M., Garcia-Franco M., Guinea J.,
563 Kluever N., Schirmer K. and Tanneberger K. (2013). A European perspective on alternatives
564 to animal testing for environmental hazard identification and risk assessment. *Regul. Toxicol.*
565 *Pharmacol.* 67: 506-530.

566
567 Shah S.Z.A., Zhao D., Khan S.H. and Yang L. (2015). Regulatory mechanisms of
568 endoplasmic reticulum resident IP3 receptors. *J. Mol. Neurosci.* 56: 938-948.

569
570 Tsamandouras N., Rostami-Hodjegan A. and Aarons L. (2015). Combining the ‘bottom
571 up’and ‘top down’approaches in pharmacokinetic modelling: fitting PBPK models to
572 observed clinical data. *Br. J. Clin. Pharmacol.* 79: 48-55.

573
574 Winiwarter S., Bonham N.M., Ax F., Hallberg A., Lennernäs H. and Karlén A. (1998).
575 Correlation of human jejunal permeability (in vivo) of drugs with experimentally and
576 theoretically derived parameters. A multivariate data analysis approach. *J. Med. Chem.* 41:
577 4939-4949.

578
579 Wishart D.S., Knox C., Guo A.C., Shrivastava S., Hassanali M., Stothard P., Chang Z. and
580 Woolsey J. (2006). DrugBank: a comprehensive resource for in silico drug discovery and
581 exploration. *Nucleic Acids Res.* 34: D668-D672.

582
583 Zhao P., Zhang L., Grillo J.A., Liu Q., Bullock J.M., Moon Y.J., Song P., Brar S.S.,
584 Madabushi R. and Wu T.C. (2011). Applications of physiologically based pharmacokinetic
585 (PBPK) modeling and simulation during regulatory review. *Clin. Pharmacol. Ther.* 89: 259-
586 267.

587
588
589
590
591
592
593
594

595 **Figure Legends**

596 **Figure 1: Schematic representation for the Petri net of the histamine H1 receptor**
597 **signalling pathway using mEPN notation.** The Petri net describes the key relationships
598 between components of the signalling pathway system culminating in the regulation of
599 downstream transcription factor expression stimulated by the binding of a ligand to the
600 histamine H1 receptor.

601 **Figure 2: Optimised transcription factor output.** The ligand (histamine) was introduced at
602 $t = 0$ (Petri net time units) in the model simulation. Prior to $t = 0$ the model was run to steady
603 state. The model solution was fit to the data via optimisation of the conserved moieties of the
604 signalling pathway. Dotted lines represent the fold increase in transcriptional activity for the
605 relevant transcription factor observed in the transcription assays. Solid lines represent the
606 normalised model solution for the corresponding transcriptional activity as simulated by
607 luciferase dynamics.

608 **Figure 3: Transient dynamic output of the histamine H1 receptor signalling pathway**
609 **using the stochastic Petri net.** This figure illustrates the dynamic output of the stochastic
610 Petri net when a small transient perturbation to the ligand concentration is made at $t=200$
611 units, representing the pre-stimulation steady state. Dynamics are shown for model variables
612 that correspond to luciferase signals for transcription factors associated with a receptor
613 stimulation perturbation.

614 **Figure 4: Metabolic Control Analysis (MCA) of the H1 signalling pathway.** Scaled
615 concentration control coefficients as a result of MCA are plotted for the activity of five
616 transcription factors modulated by histamine H1 receptor binding. Each row of the heat map
617 numerically corresponds to a reaction term in the signalling pathway model (see
618 supplementary material). Maximum and minimum values in the heat map (white patches)
619 represent maximum sensitivity to perturbation of the reaction terms in the model depicting
620 direct transcriptional regulation rates and luciferase decay rates.

621 **Figure 5: Histamine/lisuride dose response, EC_{50} and kinetic parameters.** (A): Ligand
622 (histamine) and partial agonist (lisuride) dose-response assays used to calculate EC_{50} values.
623 (B): Immunoblotting of H1 receptor in murine organs. (C): Relative quantification of
624 immunoblot relative to HeLa cell lysates.

625 **Figure 6: Temporal tissue response predicted by PBPK modelling following doses of**
626 **lisuride.** (A): 25 $\mu\text{g/mL}$ administered intravenously. (B): 0.1 mg administered orally. Tissues
627 are labelled as follows: heart (HE), lungs (LU), kidneys (KI), liver (LI), bone (BO), brain
628 (BR), spleen (SP), small intestine (SI) and colon (CO).

629

630

631 **Table Legends**

632 **Table 1: Transcription factor changes.** Alterations in expression levels of specified genes
633 in the presence of histamine after 6 hours expressed as mean fold changes in relative
634 luciferase units with standard deviation (n=3) as determined by Signal Reporter Assay.

635 **Table 2: Kinetic parameters of lisuride and the histamine H1 receptor.** Receptor
636 activation of the H1-histamine receptor was studied with known agonist (histamine) and off-
637 target agonist (lisuride). Using these assays, each parameter was calculated using GraphPad
638 Prism.

639 **Table 3: Relative amounts of histamine H1 receptor in murine tissue calculated using**
640 **immunoblot analysis.** Values were used to calculate tissue-specific receptor scaling factors
641 for lisuride EC₅₀ values when binding to the histamine H1 receptor.

642

643

644

645

646

647

648

649

650

651

652

653

654

655

656

657

658

659 TABLES

660 Table 1

Transcription Factor	Fold change in relative luciferase units
NFAT	1.97 ± 0.063
NF κ B	2.18 ± 1.47
CREB	1.54 ± 0.027
MEF2	2.74 ± 1.31
ATF2	1.67 ± 8.99

661

662 Table 2

Parameter	Value	Standard Error	Units
<i>Min</i>	7.98 %	1.066	/
<i>Max</i>	36.55 %	0.5863	/
$\log EC_{50}$	-7.968	0.06724	mol/L
<i>n</i> (Hill coefficient)	0.8411	0.1009	/
K_d	8×10^{-9}	0.0577	mol/L

663

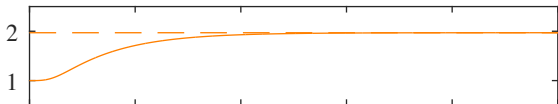
664 Table 3

Parameter	Value	Tissue
R_{HE}	5.60	Heart
R_{LU}	3.56	Lungs
R_{KI}	6.64	Kidney
R_{LI}	11.63	Liver
R_{BO}	3.88	Skeletal muscle
R_{BR}	5.78	Brain
R_{SP}	5.83	Spleen
R_{SI}	5.56	Small intestine
R_{CO}	25.90	Large intestine

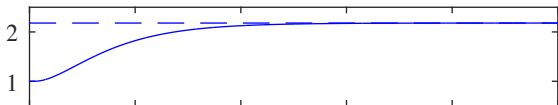
665

Luciferase Dynamics

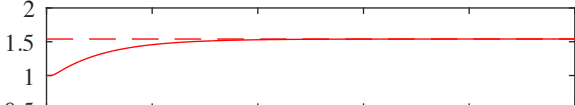
NFAT



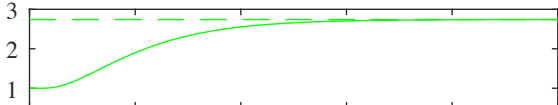
NF κ B



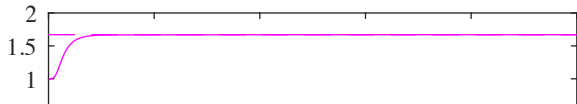
CREB



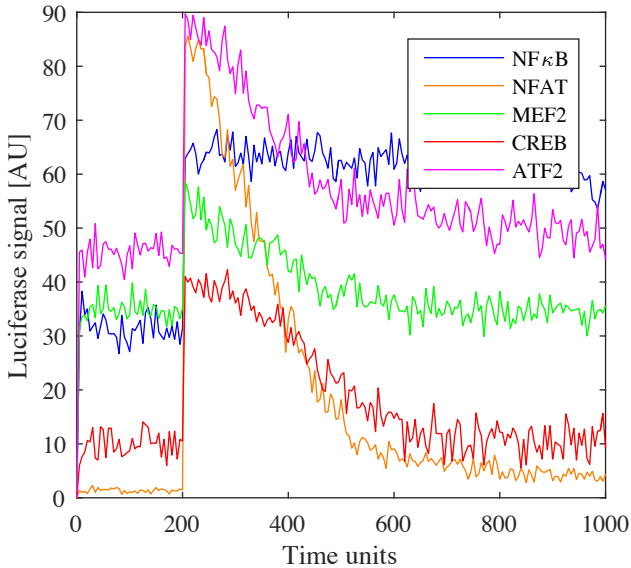
MEF2

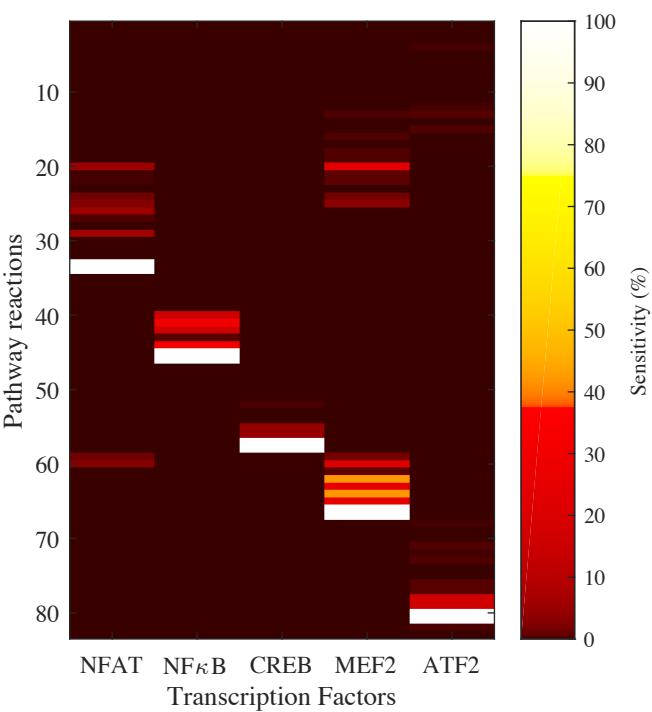


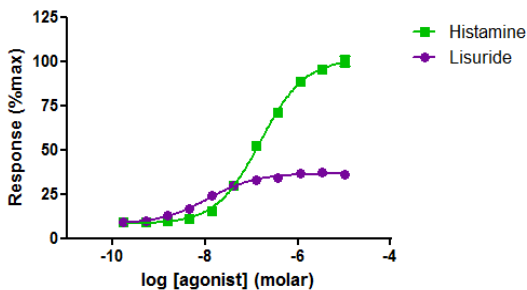
ATF2



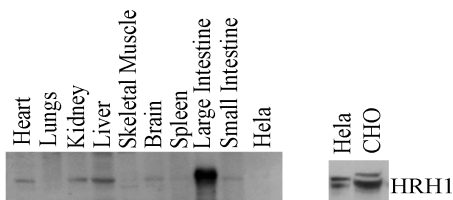
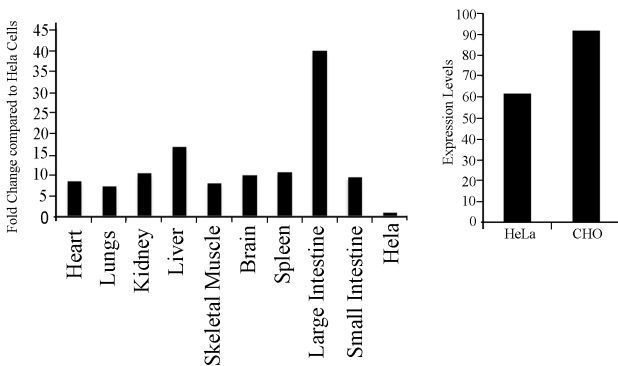
Time units

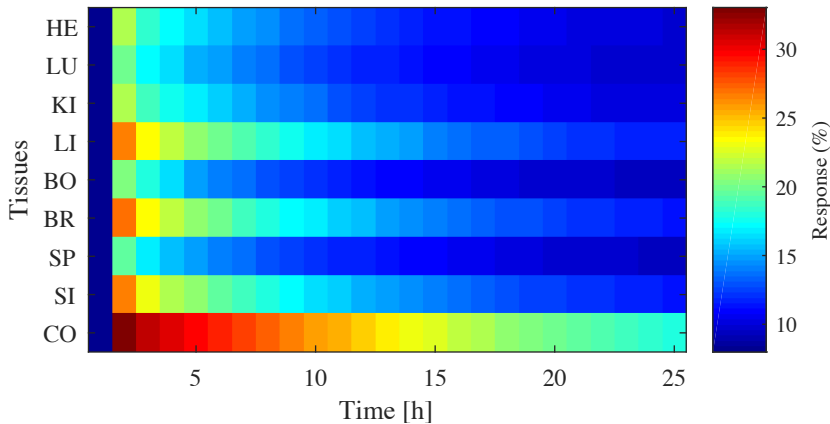




A**HRH1 Agonist Response**

	Histamine	Lisuride
HillSlope	0.9060	0.8411
EC50	1.531e-007	1.076e-008

B**C**

A**B**